

Joining Uranium to Aluminum using Electron Beam Welding and an Explosively Clad Niobium Interlayer

J. W. Elmer, P. Terrill, D. Brasher, D. Butler

This article was submitted to
54th Annual Assembly of the International Institute of Welding,
Ljubljana, Slovenia, July 8-13, 2001

U.S. Department of Energy

Lawrence
Livermore
National
Laboratory

June 12, 2001

DISCLAIMER

This document was prepared as an account of work sponsored by an agency of the United States Government. Neither the United States Government nor the University of California nor any of their employees, makes any warranty, express or implied, or assumes any legal liability or responsibility for the accuracy, completeness, or usefulness of any information, apparatus, product, or process disclosed, or represents that its use would not infringe privately owned rights. Reference herein to any specific commercial product, process, or service by trade name, trademark, manufacturer, or otherwise, does not necessarily constitute or imply its endorsement, recommendation, or favoring by the United States Government or the University of California. The views and opinions of authors expressed herein do not necessarily state or reflect those of the United States Government or the University of California, and shall not be used for advertising or product endorsement purposes.

This is a preprint of a paper intended for publication in a journal or proceedings. Since changes may be made before publication, this preprint is made available with the understanding that it will not be cited or reproduced without the permission of the author.

This work was performed under the auspices of the United States Department of Energy by the University of California, Lawrence Livermore National Laboratory under contract No. W-7405-Eng-48.

This report has been reproduced directly from the best available copy.

Available electronically at <http://www.doc.gov/bridge>

Available for a processing fee to U.S. Department of Energy
And its contractors in paper from
U.S. Department of Energy
Office of Scientific and Technical Information
P.O. Box 62
Oak Ridge, TN 37831-0062
Telephone: (865) 576-8401
Facsimile: (865) 576-5728
E-mail: reports@adonis.osti.gov

Available for the sale to the public from
U.S. Department of Commerce
National Technical Information Service
5285 Port Royal Road
Springfield, VA 22161
Telephone: (800) 553-6847
Facsimile: (703) 605-6900
E-mail: orders@ntis.fedworld.gov
Online ordering: <http://www.ntis.gov/ordering.htm>

OR

Lawrence Livermore National Laboratory
Technical Information Department's Digital Library
<http://www.llnl.gov/tid/Library.html>

Joining Uranium to Aluminum using Electron Beam Welding and an Explosively Clad Niobium Interlayer

*For submission to the 54th Annual Assembly of the International Institute of Welding
Ljubljana, Slovenia, July 8-13, 2001
Commission IV*

by
J. W. Elmer, P. Terrill, D. Brasher* and D. Butler*

Lawrence Livermore National Laboratory
University of California, P. O. Box 808, Livermore, CA, 94551

*High Energy Metals, Inc.
Port Townsend, Wa, 98368

Abstract

A uranium alloy was joined to a high strength aluminum alloy using a commercially pure niobium interlayer. Joining of the Nb interlayer to the aluminum alloy was performed using an explosive welding process, while joining the Nb interlayer to the uranium alloy was performed using an electron beam welding process. Explosive welding was selected to bond the Nb to the aluminum alloy in order to minimize the formation of brittle intermetallic phases. Electron beam welding was selected to join the Nb to the uranium alloy in order to precisely control melting so as to minimize mixing of the two metals. A Modified Faraday Cup (MFC) technique using computer-assisted tomography was employed to determine the power distribution of the electron beam so that the welding parameters could be directly transferred to other welding machines. Optical microscopy, scanning electron microscopy, microhardness, and tensile testing of the welds were used to characterize the resulting joints. This paper presents the welding techniques and processing parameters that were developed to produce high integrity ductile joints between these materials.

Introduction

A component consisting of a high strength aluminum alloy and a depleted uranium alloy was designed with the requirement of having a high integrity joint between the two alloys. This very unusual combination of materials was difficult to join because of the widely differing physical and mechanical properties between aluminum and uranium alloys. Direct fusion welding, brazing, and diffusion bonding were all initially considered for producing the joint, however, each of these joining methods had problems. A direct fusion weld was not possible due to the creation of U-Al_2 and U-Al_3 brittle intermetallic phases in the fusion zone [1]. Vacuum brazing was not possible because the aluminum-based braze alloys required to braze aluminum would also form brittle phases with the uranium at the joint interface [2,3]. Diffusion bonding of Al to U-6wt%Nb using a thin interlayer such as silver might have been possible, however, this joint would be difficult to make and its mechanical properties would not have been sufficient for the intended application [4,5].

To overcome the problems associated with making a direct joint between U-6wt%Nb and Al, we selected an intermediate metal to form the transition between them. Requirements for the intermediate metal were that it be joinable to aluminum on one side of the transition, and electron beam weldable to U-6wt%Nb on the other. Candidate materials to form the transition between aluminum and U-6wt%Nb that had the highest likelihood of success were refractory metals because many of them can be alloyed with uranium alloys. In this program, we selected niobium for this purpose since it does not form intermetallic compounds with uranium, the U-6wt%Nb alloy already contains some Nb, and the density of Nb is approximately half way between that of Al and U-6wt%Nb.

From a fusion welding standpoint, the only difficulty with joining Nb to U-6wt%Nb was that the melting point of Nb is 1329°C higher than that of uranium. However, with careful weld joint design and precision welding techniques this difference in melting points did not turn out to be a problem. The aluminum side of the joint was a bit more challenging since fusion welding and brazing of aluminum to all metals other

than aluminum alloys is difficult [2]. Therefore, it was necessary to make the aluminum side of the joint using a solid state joining process to avoid contact of liquid aluminum with the U-6wt%Nb alloy. To accomplish this, we developed an explosive welding procedure (EXW) to join the Nb to the aluminum. EXW was chosen because it is well established for aluminum alloys, and because the flat-plate geometry of the component was ideally suited for the EXW process [6].

The design of the finished component required the aluminum to be in the high strength condition. Since EXW of aluminum alloys in their low strength condition is preferred to the high strength condition, we chose to first explosively clad the Nb plate to 6061 aluminum in the solution annealed and quenched (T4) condition. This composite joint was later heat treated to bring the 6061 aluminum to the high strength -T6 condition prior to electron beam welding the clad material to the U-6wt%Nb side of the component.

This paper describes the welding techniques and processing parameters for producing both the explosively clad joint between 6061 Al and Nb, and the electron beam welded joint between U-6wt%Nb and Nb. The joints were examined using both optical metallography and scanning electron microscopy, while the mechanical properties of both the explosive weld and the electron beam weld were investigated using uniaxial tensile testing, and microhardness testing. Results showed that the mechanical properties obtained across the composite joint were similar to that of the niobium, and that these joints ultimately failed within the Nb interlayer in a ductile fashion.

Materials and Experimental Procedures

Materials

Aluminum alloy 6061 was purchased in 15-inch diameter circular pieces that were 7-inch thick. These plates were then solution anneal heat treated at 530° C for 12.5 hrs before quenching in water to place them into the -T4 heat-treated condition. The composition of the 6061 Al (wt.%) was 0.68 Si, 0.36 Fe, 0.30 Cu, 0.103 Mn, 0.93 Mg, 0.06 Cr, 0.19 Zn, 0.04 Ti, based on the mill analysis. The commercially pure Nb was purchased in annealed 15-inch square sheets, 0.375-inch thick. The composition of the Nb was 10 ppm C, 95 ppm O, 35 ppm N, <5 ppm H, 400 ppm Ta, 15 ppm Fe, and 15 ppm Si, based on the mill analysis. The U-6wt%Nb alloy was acquired in plate form and

had been heat treated at 200 °C for 2 hours; the composition of this plate was not measured. After explosive cladding, the aluminum was heat treated from the –T4 to the –T6 condition. This heat treating was performed in a vacuum furnace at 178°C for 8 hours, followed by a furnace cool to room temperature

Explosive Welding

Explosive welding was performed at High Energy Metals, Inc. to join the Nb plates to the aluminum alloy billets. All surfaces to be joined were ground flat to within 0.80 mm per meter with a surface finish better than 1.6 μm root-mean-square, and cleaned with an organic solvent in preparation for explosive welding. The surfaces to be joined were assembled parallel to each other using a constant standoff distance of 3 mm provided by aluminum shims as illustrated in Figure 1. To help ensure good bonding as far out on the O.D. of the aluminum billet as possible, an aluminum frame was fabricated around the aluminum billet to support the edges of the square Nb plate. A wooden box was then constructed around this assembly to contain the explosive mixture above the Nb plate.

The explosives used were an ammonium nitrate – fuel oil (ANFO) based proprietary mixture. The charge load was adjusted to not exceed 9 lbs/ft², for an estimated detonation velocity of 2000 to 2400 m/s. A blasting cap was placed near one corner of the Nb plate and detonated. After bonding, a visual inspection was performed at the blast site to assess edge deformation and relative flatness of the joint. Ultrasonic inspections were then performed in accordance to ASTM A578M-96 to assess the quality of the bond.

Electron Beam Welding

Electron beam welding was performed at Lawrence Livermore National Laboratory using a 150 kV/50 mA Hamilton Standard welder (No. 175) fitted with a ribbon filament and an R-40 gun. A 10 mA, 100 kV sharp-focused electron beam was used to weld the parts in a vacuum chamber pumped down to 10⁻⁵ torr. The parts were located 7.0 inch below the top of the vacuum chamber, and the weld was made by

moving the parts at a constant travel speed of 40 ipm beneath the stationary electron beam.

In order to minimize mixing between the Nb and U-6wt%Nb, a weld joint design was developed with a 70° angle to help match the natural wedge shape of the electron beam fusion zone to the U-6wt%Nb alloy that was being melted. In this design, the electron beam was concentrated on the U-6wt%Nb side of the joint in order to melt the U-6wt%Nb and allow it to wet the higher melting point Nb. This weld joint design helped to mitigate the large difference in melting points between the Nb (2469°C) and U-6wt%Nb (1140°C) and minimize mixing of the Nb with the U-6wt%Nb.

A schematic drawing of the joint design is shown in Figure 2, indicating the location of the electron beam, which is offset 0.5 mm from the location where the Nb and U-6wt%Nb come together on the top surface of the plates. This amount of offset was chosen from the results of several practice welds, which showed that the molten U-6wt%Nb may not wet the entire Nb interface to the top of the joint if the beam is offset more than 0.5 mm from the interface with these welding parameters, and that undesired melting of the Nb occurred if the offset was less than 0.5 mm.

The power density of the electron beam was measured using a Modified Faraday Cup (MFC) device [7-8]. The MFC design contained 17 slits, one measuring 0.2 mm wide and the other 16 measuring 0.1 mm wide [8]. Data was taken while scanning the beam over the MFC at 60 Hz and in a 25 mm diameter circle over the slit disk using the on-board deflection coils of the electron beam welder. Electron beam profile information was gathered as the electron beam passed over each slit by measuring the voltage drop across a 200 Ω resistor. Rapid data collection was performed using an analog-to-digital converter sampling at a frequency of 500 kHz. Figure 3a shows one of the 17 profiles taken, indicating that the data was very clean and virtually free of electronic noise. No filtering was required prior to tomographically reconstructing this data using the LLNL developed software written on LabView 5.0 [7]. Figure 3b shows the tomographically reconstructed power distribution of the electron beam, which has a nearly circular Gaussian shape with a FWHM value of 0.208 mm, a 1/e² value of 0.342 mm, and a peak power density of 20.5 kW/mm².

Materials Characterization

Optical metallography was performed on all samples using conventional polishing and etching techniques, and the samples were viewed in both the as polished and etched conditions. The Al/Nb samples were etched in a chemical bath of glycerol (20 ml), hydrofluoric acid (10 ml), and nitric acid (10 ml). Due to the difference in etching behavior between these two metals, the aluminum etched more rapidly than the Nb, leaving the Nb under-etched in most of the micrographs. The U-6wt%Nb /Nb samples were electrolytically etched in a 10% oxalic acid bath, which etched the U-6wt%Nb side of the joint more aggressively than the Nb side of the joint. Photographs of the microstructures were taken under both normal and polarized light conditions. Scanning electron microscopy was performed using a 5 keV beam to show the detail of the explosive weld interface. These micrographs were taken with the SEM in the backscatter mode to reveal the location of the Al and Nb phases, where the Nb-rich areas appear light and the Al-rich areas appear dark in contrast.

Microhardness measurements were made on polished samples using a diamond pyramid hardness (DPH) tester. Hardness measurements near weld interfaces were made using a 50 gf load, whereas bulk hardness measurements were made using a 300 gf load. The hardness measurements were calibrated using a standard test block with a 704 ± 8 DPH value at 300 gf loads. The microhardness measurements made near the interface at the lower load level of 50 gf can only be used for relative hardness values since these data were uncalibrated.

Tensile testing was performed on 1.5 mm thick dog-bone shaped tensile bars. All tests were performed using a crosshead rate of 1.3 mm/min and run at room temperature. A 50% strain extensometer with 5.0 mm gage length was used to measure strain across the explosive welded joint, while a 50% strain extensometer with a 25.4 mm gage length was used for the base metal samples and the samples containing the electron beam welds. Scribe lines were placed on all samples for elongation to failure measurements. A Micro-Measurements model 1120 signal conditioning amplifier was incorporated to provide the signal output for the extensometers, which were then used for elastic modulus and yield strength determination. All tests were performed using an Instron 1125 electro-mechanical test machine with a 1000 lb load cell, and the data was acquired with a

National Instruments PC-based data acquisition system. Elongation and cross sectional measurements were taken using a Nikon optical comparator before and after testing.

Results and Discussion

Explosive Welding 6061Al to Nb

One of the 15-inch diameter explosively clad billets was cross-sectioned to determine the quality of the joint. Figure 4 shows photomicrographs taken from this joint viewed from two different orientations: a) perpendicular to the wave front propagation, and b) parallel to the wave front propagation. The view perpendicular to the explosive front (Figure 4a) shows the wave-like nature of the explosive bond interface. Here the Nb has formed into waves above, what appears to be, a mixed region containing both aluminum and niobium constituents. This mixed region resides on a relatively flat base of aluminum. The view parallel to the explosive front (Figure 4b) shows these same regions, but does not reveal the periodic wave-like nature of the interface. Ostensible isolated islands of Nb observed in this view are most likely the cross-sectioned crests of the Nb waves that were seen in Figure 4a.

The optical micrographs indicate that some degree of mixing occurs between the Nb and the 6061 Al plates during the explosive bonding process. This mixed region was investigated further at higher magnifications using scanning electron microscopy. Figure 5 shows the results of one of these SEM micrographs, where Nb appears as high intensity regions (light areas) and aluminum appears as low intensity regions (dark areas). This SEM micrograph reveals an interfacial region that is complex, containing a mixture of large, relatively unaffected Nb pieces, and a dispersion of smaller, sub-micron sized, Nb-rich particulates. These small Nb-rich particulates have irregular shapes and oftentimes have non-smooth surfaces. The origin of the dispersed Nb phase has not been evaluated at this time, and will require additional characterization to determine its microstructural evolution.

The thickness of the interfacial region was measured at different locations from the point of detonation and was shown to be the thickest (40 μ m) close to the detonation initiation area and to be thinnest (5 μ m) near the far edge of the plate. This non-uniformity is not thought to be a problem for the intended application, however,

additional EXW experiments are being considered where the explosive is detonated from the center of the plate, in order to minimize the variation in the interfacial region thickness.

Microhardness measurements were made through the joint region in both the as explosively clad condition and also in the heat-treated condition. The 6061 Al prior to heat treating (-T4 condition) had a hardness of 95 DPH and after heat treating (-T6 condition) had a hardness of 115 DPH. These bulk hardness measurements were made using a 300 gm load. A hardness gradient was observed in the commercially pure Nb adjacent to the EXW bond line. Figure 6 shows the results of a microhardness traverse through the Nb using a 50 gm load. At the bond line the hardness of the Nb was measured to be 130 DPH, and this value decreased to the base metal value of 110 DPH at a distance of approximately 1.5 mm from the bond line.

Electron Beam Welding U-6wt%Nb to Nb

Figure 7a shows a metallographic cross section made from the welded joint at low magnification. The weld is free of cracks, free of porosity, and the weld penetration exceeded the depth of the step by 0.36 mm. It is clear that the fusion line followed the 708 angle of the original joint preparation on the Nb side of the weld, showing minimal dissolution of Nb into the fusion zone. The entire Nb interface was wet by the molten U-6wt%Nb alloy, which left no undercut on the top surface of the weld joint. The final part could then be machined from the completely fused portion of the weld above the step in the joint.

Figure 7b shows a close up view of the Nb side of the fusion zone, indicating perfect wetting of the Nb interface by the molten U-6wt%Nb alloy. Dendritic solidification occurred on this side of the joint with epitaxial growth occurring from the Nb base metal/U-6wt%Nb interface. Figure 7c shows a close up view of the U-6wt%Nb side to the fusion zone, indicating that the molten U-6wt%Nb alloy solidified in a cellular/dendritic mode with epitaxial regrowth from the U-6wt%Nb base metal.

Microhardness measurements were made in and around the U-6wt%Nb/Nb electron beam welded joint to determine if any hard phases were formed in the fusion zone and to determine if any softening occurred on either side of the joint. The hardness

of the U-6wt%Nb alloy was measured to be 220 DPH in the base metal, 180 DPH in the HAZ, and 240 DPH in the middle of the fusion zone of the electron beam weld. The Nb, adjacent to the electron beam weld measured 104 DPH. Thus the fusion zone had a hardness very similar to that of the base metal U-6wt%Nb, and some softening occurred in the HAZ on both sides of the electron beam weld.

Tensile Test Results

Tensile tests were performed on the base metals and on the joined dissimilar metal combinations. All samples that contained welds were prepared as cross-weld tensile samples with the weld running perpendicular to the tensile axis, as illustrated in Figure 8. The 25.4 mm extensometer was used to measure the strain on all of the base metal samples for the tensile bar configuration shown in Figure 8a. The 5.0 mm gage length extensometer was used to measure the strain of the explosively welded Nb/Al joint, for the joint configuration schematically shown in Figure 8b.

Figure 9 plots representative stress-strain curves for the different base metals, and these results are summarized in Table 1. The Nb is the most ductile of the base metals and exceeds 10 % elongation at failure as measured using scribe lines placed 25 mm apart. The Nb was shown to have a gradient in properties, being stronger and harder near the bond line than in the parent metal. Tensile samples removed parallel to the explosive bond and from a region within 2 mm from the bond line had a yield strength of 46.9 ksi, which is 15 % higher than that of the Nb base metal (40.6 ksi).

The effect of heat-treating on the properties of the aluminum alloy was studied by pulling tensile bars in the as received, -T4, condition and in the heat treated, -T6, condition. Before heat-treating the yield strength of the 6061 Al measured 33.6 ksi. After heat treating the yield strength of the aluminum increased to 41.9 ksi, which is similar to the yield strength of the Nb base metal. The ultimate strength of the 6061 AL-T6 and Nb are also similar and are both approximately 45 ksi, however, the ultimate strength of the U-6wt%Nb is significantly higher at 130.4 ksi. The aluminum in the -T6 condition and the U-6wt%Nb are the least ductile base metals, having elongations at failure of 6.4 and 6.2 % respectively as measured using scribe lines placed 25 mm apart. The modulus of elasticity of the 6061 Al was measured to be 10.3 Msi, which is about 30

% lower than that of the Nb (13.2 Msi), and slightly higher than that of the U-6wt%Nb (9.8 Msi).

Figure 10 compares the tensile curves of the cross weld samples with that of the Nb base metal. In all cases the welded joints failed in the Nb in a ductile manner. These results clearly indicate that, in these mis-matched joints, the Nb is the softest material and receives the majority of the deformation. The tensile curves for the welded joint were acquired using only one extensometer, and therefore do not account for the individual localized strains that develop on either side of the joint [9]. However, the stress strain curves shown here do provide useful information regarding the overall behavior of these joints, and thus provide an indication of how well the joints will perform in service.

Tensile bars consisting of Nb/6061Al-T6 taken from the explosively welded joint were tested with the joint configuration illustrated in Figure 8b. These samples failed in the Nb and had an average yield strength of 39.7 ksi, which is very close to that of the Nb base metal strength (40.6 ksi). The ultimate strength of this joint measured 47.1 ksi, which was slightly higher than that of the Nb base metal (44.9 ksi). The elongation of this joint, as measured by 5 mm wide scribe lines placed on the sample, measured 39.5% elongation at failure. This elongation is significantly larger than that indicated by the stress strain curve shown in Figure 10 and higher than that measured on the base metal samples. These differences are due to a combination of the smaller gage length of the scribe lines than those used on the base metal samples and the fact that the failure occurred outside the gage length of the extensometer.

The U-6wt%Nb/Nb tensile bars from the electron beam welded joint were separately tested using the joint configuration shown in Figure 8c. The average yield strength of these welds measured 31.1 ksi and failure occurred on the Nb side of the joint. This lowered yield strength is the result of the electron beam weld, which had an annealing effect and reduced the strength of the Nb. The ultimate strength of this joint measured 37.1 ksi and the joint had an average elongation to failure of 11.5% as measured with 25.4 mm wide scribe lines.

The complete joint containing both an electron beam weld and an explosive weld was tensile tested after heat treating the aluminum to the -T6 condition. These U-6wt%Nb/Nb /Al-T6 tensile bars were tested with the joint configuration shown in Figure

8d, and all samples failed in the Nb interlayer. The average yield strength of these welds was 34.7 ksi, which is 15% lower than that of the Nb base metal. This lowered yield strength is again the result of the electron beam weld, which had an annealing affect on the explosively clad Nb interlayer and thus softened the overall joint. The ultimate strength of this joint still remained high at 45.0 ksi, and is similar to that of the Nb base metal (44.9 ksi). The ductility of this joint, as measured by 10 mm wide scribe lines placed on the sample, measured 21.0 % elongation at failure. This elongation is again higher than that measured on the base metal due to the combination of strain concentration in the softer Nb and the use of smaller gage length scribes lines than were used for the base metal tests.

Table 1: Summary of the tensile and hardness properties measured on the base metals and on the completed joints.

Material	Hardness (DPH)	No. tests	$\sigma_{y, 0.2\%}$ (ksi)	σ_{UTS} (ksi)	Elon. (%)	E (Msi)	Failure
Base Metals							
6061 Al-T4	95	2	33.6	40.2	8.2**	10.2	-
6061 Al-T6	115	2	41.9	45.2	6.4**	10.3	-
Nb, at the bond line	130	2	46.9	48.1	12.9 **	12.2	-
Nb,>3 mm from bond line	105	6	40.6	44.9	17.1 **	13.2	
U-6wt%Nb	220	2	44.8	130.4	6.2**	9.8	-
Welds							
Nb/AL-T6	-	3	39.7	47.1	39.5 *	13.1	Nb
U-6wt%Nb/Nb	-	3	31.1	37.1	11.5 **	9.93	Nb
U6wt%Nb/Nb/6061Al-T6	-	3	34.7	45.0	21.0 ***	13.8	Nb

* 5 mm G.L., ** 25 mm G.L., *** 10 mm G.L.

Summary and Conclusions

A method for joining 6061 Al to U-6wt%Nb was developed using a Nb interlayer between the two alloys. To do this, an explosive welding procedure was developed to join a 0.375-inch thick Nb plate to a 6061 Al billet. The explosive welding procedure minimized the formation of brittle phases between Nb and Al, and was performed with the Al initially in the –T4 condition to facilitate explosive welding. The resulting joint between the Nb cladding and the 6061 Al-T4 was well bonded as verified through ultrasonic testing. Rough machining of the Nb clad aluminum joint was then performed, and afterwards, the part was heat treated to put the 6061 Al into the high strength –T6 condition. Following heat-treating, the fusion weld joint details were machined into the Nb cladding, and it was electron beam welded to the U-6wt%Nb alloy part. The component was then final machined from this tri-metallic part. Tensile tests, microhardness measurements and metallographic characterization were performed on the joined components, and the following conclusions were made :

- 1) Commercially pure Nb can be explosively clad to 6061 Al. The resulting bond is strong, easily machined, and can be used to provide a transition between aluminum and other materials.
- 2) During explosive welding, the strength and hardness of the Nb increase. This effect was observed only within the first 1.5 mm from the explosive weld interface where the yield strength was observed to increase approximately 15% above that of the base metal.
- 3) Explosive welding of Nb to Al worked well for the 6061 Al in the –T4 condition. Heat treating the Nb clad Al billet from the –T4 condition to the –T6 condition was performed after explosive welding, and did not adversely affect the strength of the explosive bonded joint.
- 4) A method for electron beam welding U-6wt%Nb to Nb was developed. This method used a beveled joint design and concentrated the electron beam into the lower melting point U-6wt%Nb alloy to minimize mixing of the two metals. The

resulting fusion zone did not display any brittle phases, and had hardness values similar to that of the U-6wt%Nb base metal.

- 5) The final tri-metal joint contained both an explosive weld and an electron beam fusion weld. Tensile tests across this joint showed that the joint always failed in the Nb interlayer, and had a yield strength of 34.7 ksi. This yield strength is somewhat lower than that of the Nb base metal due to the annealing effects of the electron beam weld on the Nb interlayer material.

Acknowledgments

This work was performed under the auspices of the U. S. Department of Energy, Lawrence Livermore National Laboratory, under Contract No. W-7405-ENG-48. The authors would like to express their gratitude to many LLNL employees who contributed to this project, including Mr. Alan Teruya for assisting with the electron beam diagnostics, Mr. Mark Gauthier for making the electron beam welds, Mr. Robert Kershaw and Mr. Bob Vallier for optical metallography and microhardness testing, Mr. Jim Ferriera for scanning electron microscopy, and Mr. Dave Hiromoto for tensile testing.

References

1. Binary Alloy Phase Diagrams, Second Edition, Vol. 3, T. B. Massalski editor in chief, *ASM International*, 1990.
2. ASM Metals Handbook: Welding, Brazing and Soldering, Vol. 6, *ASM International*, p. 937, 1993.
3. Brazing, M. Schwartz, *ASM International*, 1987.
4. R. S. Rosen, D. R. Walmsley and Z. A. Munir, "The Properties of Silver-Aided Diffusion Welds Between Uranium and Stainless Steel," *Welding Journal*, 65(4), p. 83-s, 1986
5. J. W. Elmer, M. E. Kassner, and R. S. Rosen, "The Behavior of Silver-Aided Diffusion-Welded Joints under Tensile and Torsional Loads," *Welding Journal*, 67 (7), p 157-s, 1988.
6. ASM Metals Handbook: Welding, Brazing and Soldering, Vol. 6, *ASM International*,

p. 896, 1993.

7. J. W. Elmer, A. T. Teruya and D. W. O'Brien, " Tomographic Imaging of Non-Circular and Irregular Electron Beam Power Density Distributions," *Welding Journal* 72(11), p 493-s, 1993.
8. J. W. Elmer and A. T. Teruya, "Fast Method for Measuring Power-Density Distribution of Non-Circular and Irregular Electron Beams," *Science and Technology of Welding and Joining*, 3(2), p. 51, 1998.
9. J. Naumann, J. Vogel, D. Dobi, T. Angermann and M. Koçak, " Analysis of the Elastic-Plastic Deformation Behavior of Austenitic-Ferritic Interface Cracks Using Geometric Moiré," in *Mis-Matching of Interfaces and Welds*, edited by K. –H. Schwalbe and M. Koçak, GKSS Research Center Publications, Geesthacht, FRG, pp. 247-258, 1997.

Figure Captions

1. Schematic drawing of the explosive welding setup. The cylindrical aluminum billet is clad using an oversized square Nb plate to promote good bonding near the edge of the aluminum billet.
2. Schematic drawing of the electron beam weld joint design. The beam is offset 0.5 mm into the U-6wt%Nb alloy from joint interface on the top surface of the component and a beveled joint design is employed to minimize mixing of the two alloys.
3. a) Raw data from the MFC showing one of the 17 electron beam profiles acquired for computer assisted tomographic reconstruction of the electron beam. b) Tomographically reconstructed power density distribution of the electron beam having a peak power density of 20.5 kW/mm^2 .
4. Optical metallographic cross sections of the explosive weld joint. a) shows the interface as viewed perpendicular to the explosive front direction, and b) shows the interface as viewed parallel to the explosive front direction.
5. Scanning electron microscope image taken at the Nb/Al interface. The Nb clad plate is on the left side of the micrograph and appears light in contrast in the backscattered electron image mode. The $40 \text{ }\mu\text{m}$ wide interfacial region is composed of a fine distribution of submicron Nb-rich particles with occasional large fragments of the Nb.
6. Microhardness traverse through the explosively clad Nb interlayer, showing an increase in hardness within 1.5 mm of the explosively bonded interface.
7. a) Optical metallographic cross section of the electron beam weld fusion zone at low magnification. The U-6wt%Nb alloy is on the right hand side of the micrograph, revealing a fusion zone shape consistent with that of a keyhole penetration mode weld. The Nb is on the left hand side of the micrograph, revealing the largely unmelted 70° angled joint preparation. b) High magnification micrograph of the Nb side of the fusion zone, and c) high magnification micrograph of the U-6wt%Nb side of the fusion zone.

8. Schematic drawing of the different tensile bar configurations. A) base metal sample, b) explosive weld sample, c) electron beam weld sample, and d) explosive and electron beam weld sample.
9. Tensile curves for the base metals of U-6wt%Nb, Nb, and the aluminum in both the heat treated and in the solution annealed and quenched conditions.
10. Tensile curves for the welded samples are compared to the Nb base metal.

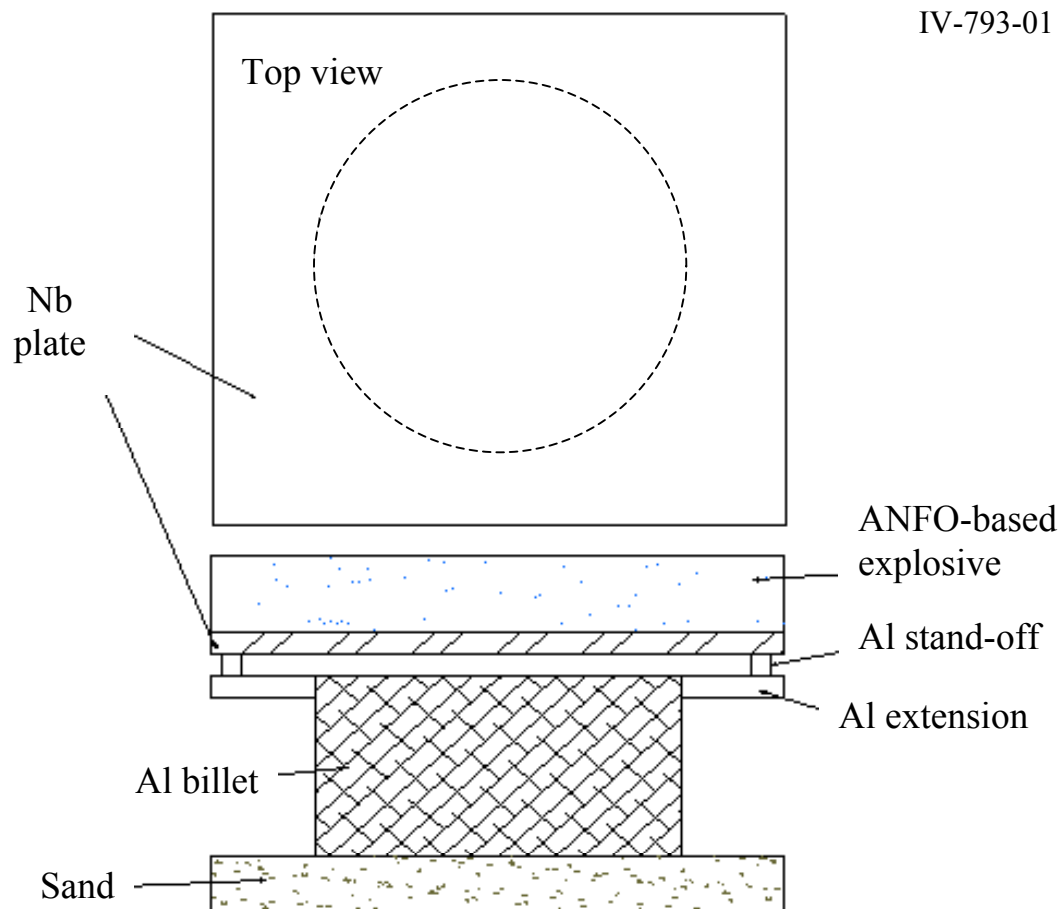


Figure 1: Schematic drawing of the explosive welding setup. The cylindrical aluminum billet is clad using an oversized square Nb plate to promote good bonding near the edge of the aluminum billet.

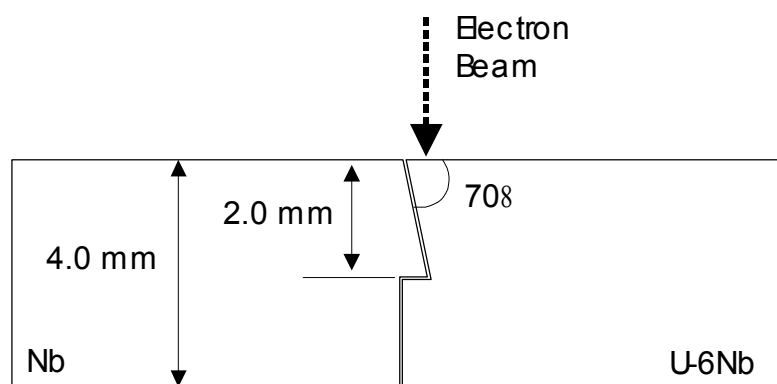


Figure 2: Schematic drawing of the electron beam weld joint design. The beam is offset 0.5 mm into the U-6wt%Nb alloy from joint interface on the top surface of the component and a beveled joint design is employed to minimize mixing of the two alloys.

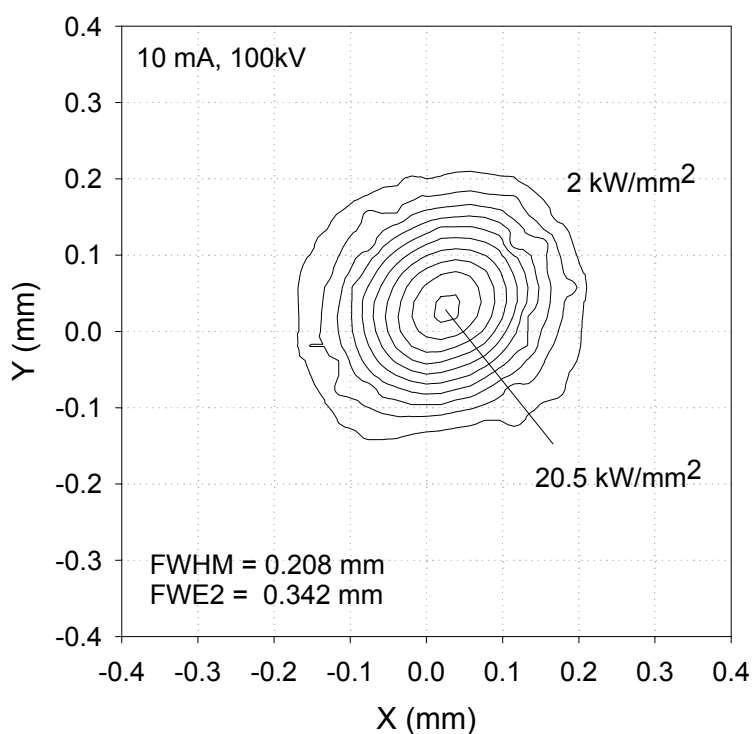
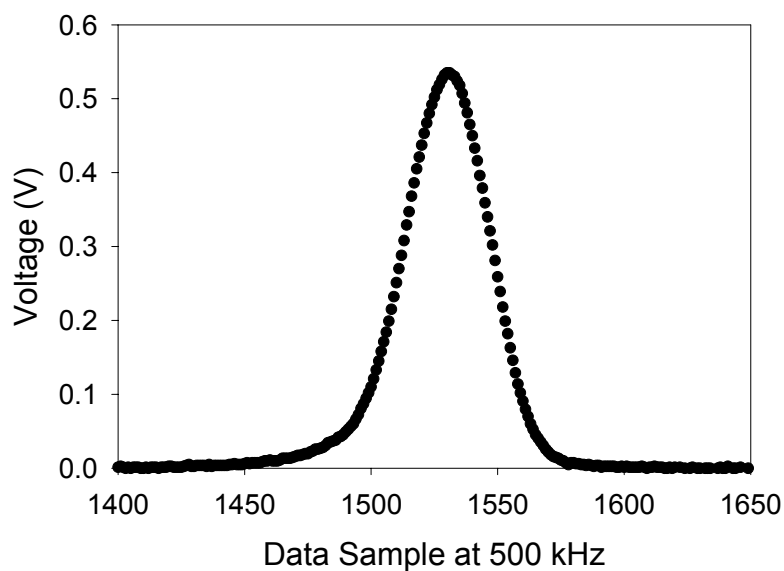


Figure 3: a) Raw data from the MFC showing one of the 17 electron beam profiles acquired for computer assisted tomographic reconstruction of the electron beam, showing a smooth profile with minimal electronic noise. b) Tomographically reconstructed power density distribution of the electron beam having a peak power density of 20.5 kW/mm^2 .

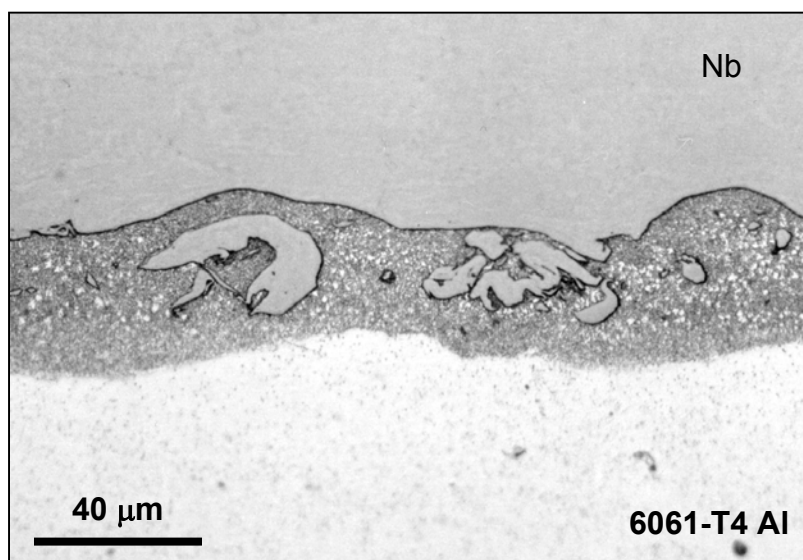
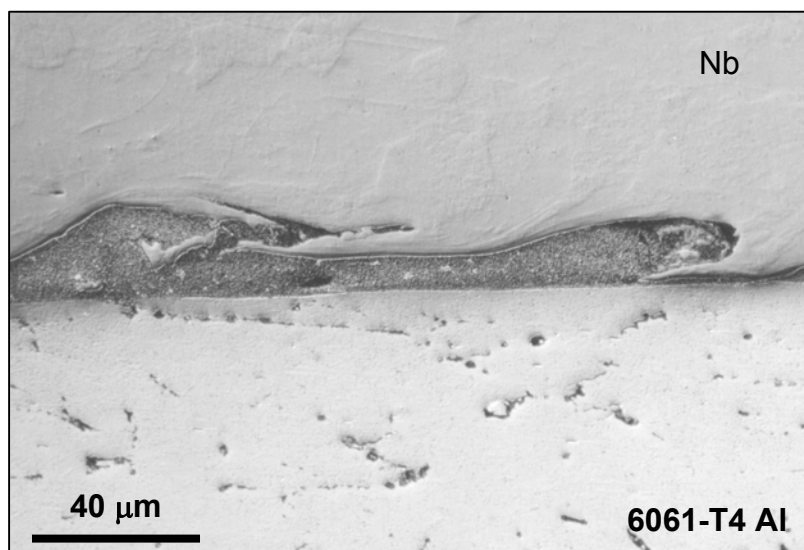


Figure 4: Optical metallographic cross sections of the explosive weld joint. a) shows the interface as viewed perpendicular to the explosive front direction, and b) shows the interface as viewed parallel to the explosive front direction.



Figure 5: Scanning electron microscope image taken at the Nb/Al interface. The Nb clad plate is on the left side of the micrograph and appears light in contrast in the backscattered electron image mode. The 40 μm wide interfacial region is composed of a fine distribution of submicron Nb-rich particles with occasional large fragments of the Nb.

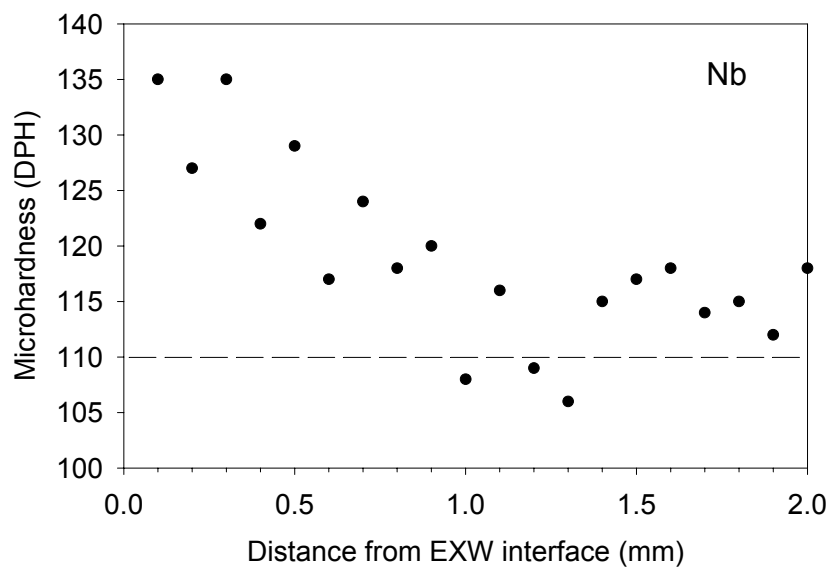


Figure 6: Microhardness traverse through the explosively clad Nb interlayer, showing an increase in hardness within 1.5 mm of the explosively bonded interface.

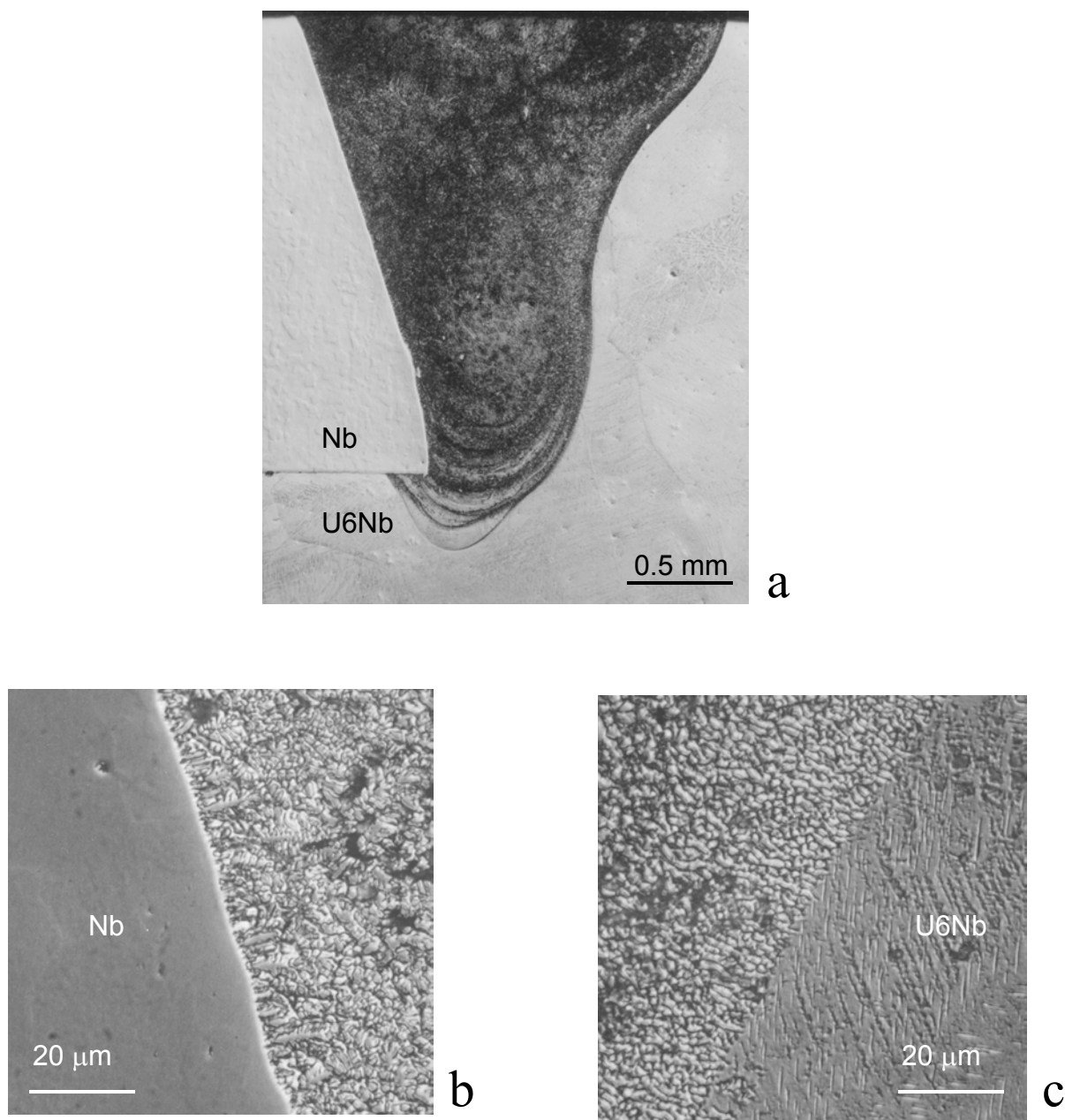


Figure 7: a) Optical metallographic cross section of the electron beam weld fusion zone at low magnification. The U-6wt%Nb alloy is on the right hand side of the micrograph, revealing a fusion zone shape consistent with that of a keyhole penetration mode weld. The Nb is on the left hand side of the micrograph, revealing the largely unmelted 70° angled joint preparation. b) High magnification micrograph of the Nb side of the fusion zone, and c) high magnification micrograph of the U-6wt%Nb side of the fusion zone.

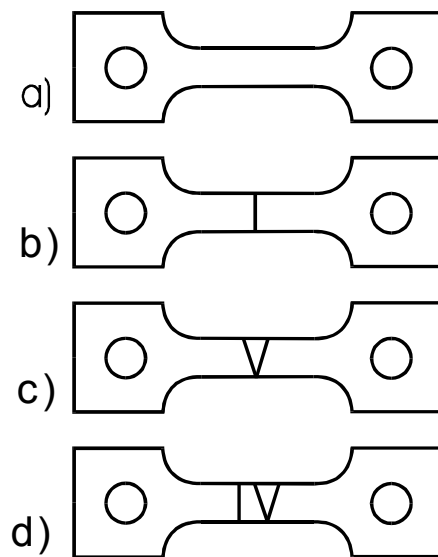


Figure 8: Schematic drawing of the different tensile bar configurations. A) base metal sample, b) explosive weld sample, c) electron beam weld sample, and d) explosive and electron beam weld sample.

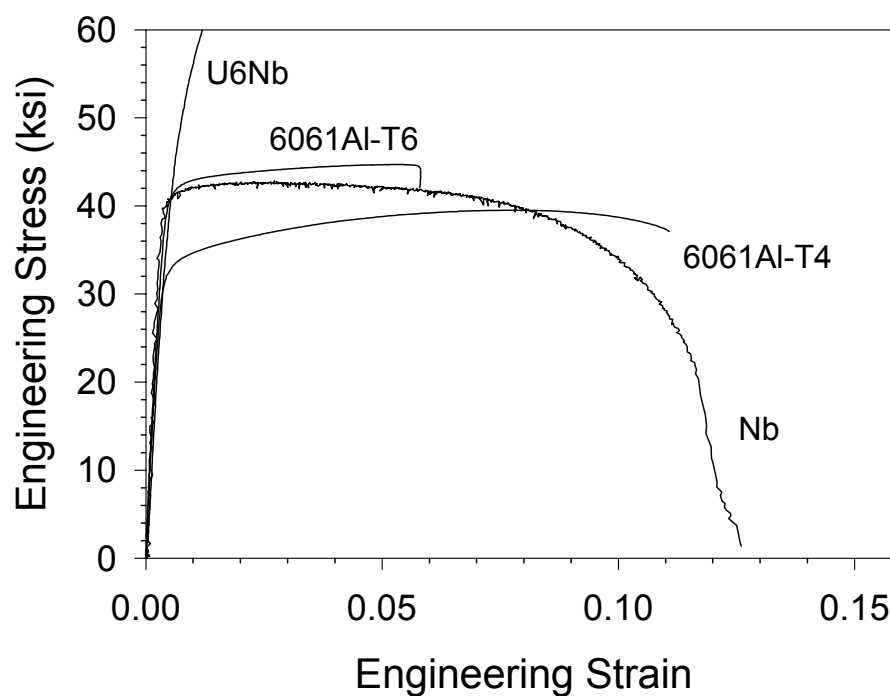


Figure 9: Tensile curves for the base metals of U-6wt%Nb, Nb, and the aluminum in both the heat treated and in the solution annealed and quenched conditions.

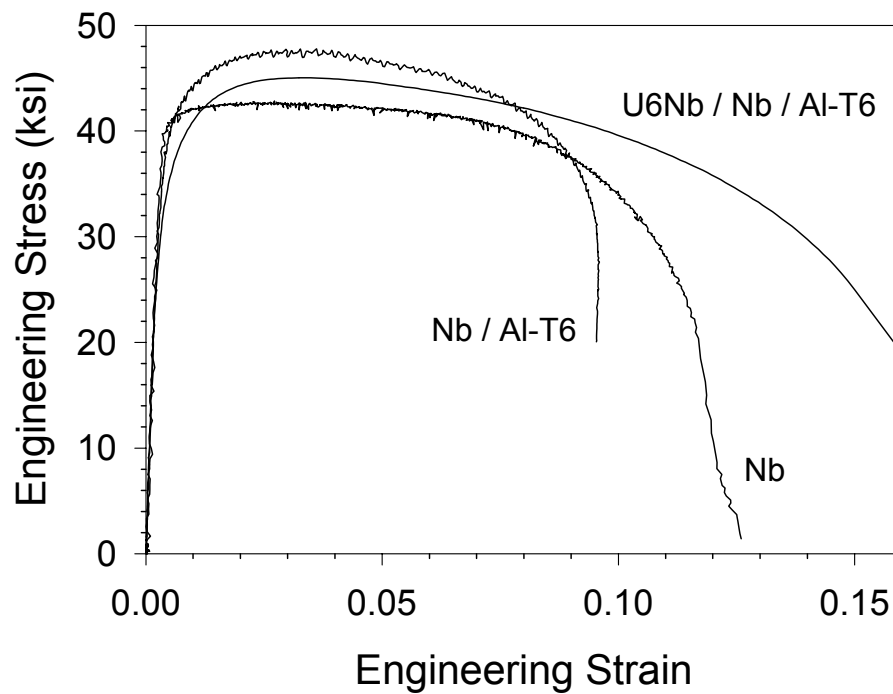


Figure 10: Tensile curves for the welded samples are compared to the Nb base metal.